A STUDY OF WATER-SURFACE DEFORMATION BASED ON 2D FLOW SIMULATION OF AN AMAZONIAN FLOODPLAIN

Sebastien Pinel[1,2,]; Taina Conchy Sampaio[1,2]; Joecila Santos Da Silva[1,2]; Marie-Paule Bonnet[3,2]*

Resumo. A augmentacao do poder computaçional e dos dados de sensoriamento remoto abriram novos horizontes para monitorar hidrológicos eventos. Tambem, existe uma necessidade no monitoramento da bacia amazônica que enfrenta uma antropização crescente e eventos hidrológicos extremos. A modelagem hidrodinâmica gera novas informações. Utilizamos um modelo 2D calibrado de uma planície de inundacao (FP) (Lago Janauacá, AM, Brasil) para analisar as Deformações da Superfície da Agua (WSD). Comecamos por validar o modelo: i) (verticalmente) correlação e NSE apresentam altos valores (0,99 para ambos); ii) (horizontalmente) as extensões de inundação são bem simulada (TS de 87), com uma tendência de superestimação (BIAS de 6). A análise da declividade no rio apresenta declividade variando ao longo do ano (declividade média de 2,55 cm.km^{-1}). Na FP, as WSD observadas (∓49 cm) são maiores do que as simuladas (∓11 cm). O modelo prevê variações de declividade importantes no canal de conexão de -0,01 cm.km^{-1} para 19,61 cm.km^{-1}. No entanto, o último valor provavelmente é superestimado, pois o modelo não simula a desconexão entre o rio e a FP que realmente acontece. No resto da FP, a WSD é inferior a 1 mm, com algumas exceções aonde as WSD alcançam 0,40 cm. O vento afeta principalmente as elevações no lago: de 0,4 cm a 1,4 cm durante agua alta.

Palavras-chave: Amazonas, hydrodynamica, Deformacão da surface de agua.

A STUDY OF WATER-SURFACE DEFORMATION BASED ON 2D FLOW SIMULATION OF AN AMAZONIAN FLOODPLAIN

Abstract. The growing availability of the computing power and remotely sensed data has opened new horizons for monitoring hydrological events. In Parallel, there is needs in monitoring the Amazonian Basin, which is facing increasing anthropization and extreme flood events. We use a calibrated 2D model of an Amazonian FP (Janauacá Lake, Amazon state, Brazil) to analyze the water-surface deformations (WSD). Firstly, we validate the model: i) (vertically) correlation and NSE present high values (0.99 for both ones); ii) (horizontally) the model well succeeds in retrieving the flood extents (TS of 87), with a slight trend to overestimation (BIAS of 6). The slope analysis in the mainstream of the study zone reports slopes varying along the hydrologic year (averaged slope of 2.55 cm.km^{-1}). In the FP, the range of observed WSD (∓49 cm) is higher than the simulated ones (∓11 cm). The model predicts important slopes variations in the connecting channel from -0.01 cm.km^{-1} to 19.61 cm.km^{-1}. Nevertheless, the latter value is likely overestimated as the model does not provide the full disconnection between the mainstream and the FP that happens. In the rest of the FP, WSD are below 1 mm, except for some exceptions where WSD reaches 0.40 cm. The wind mainly impacts the elevations in the lake: from 0.4 cm to 1.4 cm at HW.

Keywords: Amazon; Hydrodynamics; Water-surface deformation;

[1] RHASA, Universidade Estadual da Amazonas, Caixa Postal 69050-020 - Manaus – AM, Brasil, sebpinel@gmail.com, jsdsilva@uea.edu.br, tainaconchy@gmail.com

2 Institut de Recherche Laboratoire Mixte International, LMI OCE « Observatoire des changements Environnementaux », Institut de Recherche pour le Développement / Universidade de Brasilia, Campus Darcy Ribeiro, Brasilia, Brazil, marie-paule.bonnet@ird.fr

3 UMR 228 ESPACE-DEV - Institut de Recherche pour le Développement/Université de la Guyane – Maison de la teledetection, Montpellier, France

*Autor Correspondente : Sebastien Pinel; sebpinel@gmail.com; Tel.: +55-61-99827-5286

1. INTRODUCTION

Today, the growing availability of computing power, of storage data, and of fine spatial and temporal resolution data, the proliferation of remote sensing has increased the opportunities for flood modelling. Since 1998, the Copernicus program (ESA, 2016), aims at providing continuous and accurate EO data. The on-going Mission (e.g. Sentinel, MODIS, Landsat), the numerous studies (reviewed in Grimaldi *et al.*, 2016; Pinel *et al.*, 2017, In submission) on integrating remote sensing with floods modeling spotlight there is a will of scientific community to fortify the support satellite missions can offer over water monitoring.The future NASA–CNES–CSA Surface Water and Ocean Topography (SWOT) satellite mission will be launched in 2020. It will deliver maps of water-surface elevation, slope and extent with an unprecedented resolution of 100 m (Biancamaria *et al.*, 2016). This mission was planned to compensate for the lack of relatively high-resolution global datasets characterizing continental surface water storage. It will thus provide observations of rivers wider than 100 m and large water-surface areas between 78° S and 78° N. In hydrology, the SWOT satellite data will be a crucial tool for complicated issues, such as water resource management, hydrodynamics modeling, or global hydrological modeling (Paiva *et al.*, 2015). Before its launch, scientific studies must be carried out to report on the possibilities of using SWOT products in fields such as hydrology. This will help in making critical decisions, such as the choice of the satellite orbit for the validation/calibration phase.

In the large unmonitored region, such as the low Amazonian basin, EO data appear as a solution to gather input data towards monitoring. Amazonian Floodplains (FP) play an major role in the spread of flows (Paiva *et al.*, 2012), in sediment transfer (Mangiarotti *et al.*, 2013), and in the cycles of chemical elements (Bonnet *et al.*, 2016). They are considered as diversity hotspots (Junk *et al.*, 2004). Today, these sensitive zones are facing increasing human anthropization: expansion of the agricultural, mining, oil and hydroelectricity sectors (Nepstad *et al.*, 2014). This development also goes with population increase (IBGE, 2016). Combined with global warming and a spatiotemporal redistribution of precipitation (Nobre *et al.*, 2013), land-use changes across Amazonia have resulted in widespread loss of soils, biodiversity and marked shifts in biogeochemical cycles. Changes in precipitation are already observed through an augmentation in frequency and intensity of extreme hydrological events (droughts in 2005, 2010, floods in 2009, 2012, 2014) (Marengo *et al.*, 2011). Hence, there is a crucial need to monitor these Amazonian wetlands.

This work aims to study the water-surface deformations (WSD) that occur over the Janauacá FP. To this purpose, we use the simulation of a model calibrated for the zone in a previous work (Pinel *et al.*, in submission). Firstly, we validate the model in terms of vertical and horizontal accuracy. The WSD analisys initiate by the study of the slopes in the mainstream. Then, we focus in the FP comparing the results given by observed (in situ and altimetrics data) and the simulated data. The latter also permit exhibiting the evolution of the WSD along an hydrological year. Finally, we investigate the wind influence over the WSD in the FP.

2. METHOD

1.1. Study site

The Janauacá FP (Fig. 1) is located in the central zone of the Amazon Basin (AB) between 3.200°S-3.250°S and between 60.23°W-60.13°W. The Janauacá FP is composed of one lake with fringing flooded forests linked to the Solimões River by a perennial channel, denoted connecting channel (CC). In the southern part of the basin, Bonnet *et al.*, (2017) assimilated the FP to a “south stream”zone (SS). According to rainfall data in Manacapuru (3.31°S, 60.58°W), at about 40 km upstream, the mean annual rainfall over the region is 2272 $mm.yr^{-1}$. The mean of the mainstream (Solimões River) fluctuations reaches 9.85 m, at the Manacapuru WL gauge. The mainstream has a mono-modal flood phase usually starting rising mid-November until mid-June.

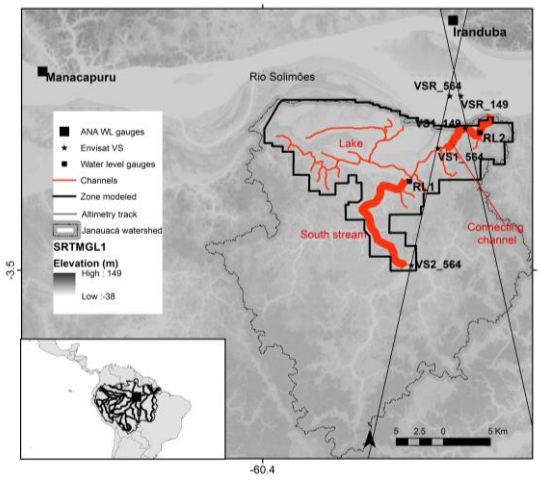

Fig. 1. Study site centered on Janauacá FP and its local drainage basin with the locations of available river stage gauges and the rainfall gauges with background SRTMGL1

1.2. Material

1.2.1 The calibrated model

The IPH-ECO model (Fragoso *et al.*, 2009) is a 3D hydrodynamic module coupled with an ecosystem module (www.ipheco.org). The hydrodynamic module solves the Navier–Stokes equations using a semi-implicit discretization. In this study, **we use a 2D model simulating** the 11/10/2006-08/31/2008 period. We restrict the modelled domain to the maximum floodable area (Fig. 2) and the spatial resolution to 93 m. The model requires boundary conditions (BC): i) water flow BC at the outlets of the local sub-basins; ii) WL BC along cells in contact with the mainstream. **The calibration needs** to drop down the resolution (278 m) to make several runs. Simulated WL at RL1 and RL2 during the first hydrologic year are analyzed to calibrate. Based on a wetlands map (Hess *et al.*, 2015), we establish a land cover map of 4 zones. We disturb common Mannings (Arcement Jr & Schneider, 1989). It leads to coefficients of 0.032, 0.042, 0.14 and 0.18 for the water/herb, shrubs, flooded forest, and *terra firme* zones, respectively.

1.2.3 Validation data

The altimetry (ENVISAT/RA-2) provides 3 VS (with a time step of 35 days): VS1_564, VS2_564, VS1_149 **(Fig. 2)**. The quality of the Envisat series is variable: results range from 12 cm to several meters. Santos *et al.* (2010) reported a positive bias of 1.044 ± 0.212 m over the AB. Hence, with 95% confidence, the accuracy of altimetrics WL is ∓ 42.4 cm.

The ANA provides two WL gauges in the Solimões River (http://hidroweb.ana.gov.br/). The fist one at Manacapuru (3.31°S, 60.58°W, labelled 14100000), is located 50 km upstream of study zone. The other one at Iranduba (3.26°S, 60.21°W, labelled 1410100) is located in front of the Janauacá lake. The estimated precision is ∓ 5 cm.

In addition, two WLs gauges were installed in the FP at "RL1" (3.42°S, 60.26°W) and "RL2" (3.36°S, 60.19°W) (Fig. 1). These gauges were leveled with the help of satellite radar altimetry level time series data. The comparison between altimetry data and *in situ* records enabled to correct or fulfil *in situ* data. The expected precision is ∓ 15 cm. we also expect this accuracy to be degradated for extreme events, as the gauges can remain under water (extreme floods 2009, 2012, and 2015) or out of water (dry events 2010, and 2016).

We extract the inundation extent from the optical Landsat 5TM and Landsat 8OLI through the normalized difference index (Xu, 2006). Pinel *et al.* (in submission) detail the method to discriminate wet pixels. They also assume that flood extent can be approximated by a DEM horizontal plane. For WL below 15 m, the DEM-predicted extent is lower than the Landsat-

predicted, while we observe the contrary for WL above 15 m. In this case, water below canopy is hardly detected by Landsat (Yamazaki *et al.*, 2015).

1.3. METHODS

1.3.1 Model validation

The vertical WL accuracy assessment consists in comparing the modeled WL against data from the 5 gauges located in the FP. We computed the following statistics: the Pearson correlation coefficient, the RMSE (m), and Nash-Sutcliffe efficiency (NSE). The horizontal accuracy is calculated using classical skills scores (Paiva *et al.*, 2011): the Threat Score (TS) and the bias index (BIAS).

1.3.2 WSD analysis

We spatially (Lake, CC, SS) and temporaly (Table 1) analyze the WSD. For each date, we compute the anomaly map based on the averaged WL at each specific date. To investigate on the wind influence, we added 4 dates corresponding to distinct hydrologic and windy conditions.

Table 1. Dates chosen for analysis of the free surface analysis

Analysis	Hydrologic period	Date	RL1 WL (m)	Average wind velocity ($m.s^{-1}$)	Wind direction
WSD along a HY	LLW	Dec-11-2007	13.92	--	--
	ERW	Feb-02-2008	17.98	--	--
	LRW	May-08-2008	21.38	--	--
	HW	May-20-2008	22.58	--	--
	FW	Aug-31-2007	18.09	--	--
	LLW	Sep-28-2007	13.94	--	--
Wind impact on WSD	LW with wind	Oct-09-2008	12.88	3.6	ESE
	LW without wind	Oct-06-2008	13.09	1.3	SSW
	HW with wind	Jul-15-2008	21.90	3.1	ESE
	HW without wind	Jul-12-2008	21.96	0.1	WSW

3. RESULTS AND DISCUSSION

1.4. Vertical and horizontal validation

Global RMSE, NSE and correlation coefficient between simulated and observed data at the fifth stations over the entire period are 0.27 m, 0.99 and 0.99, respectively (Fig. 2, Table 2). Comparing to the amplitude of the flood wave (11.60 m), RMSE value remains low. Statistics vary depending on the water period. RMSE values range from 0.48 m at LW to 0.12 m at RW. Correlation and NSE present the lowest values at LW: 0.32 and -0.40, respectively. Other FP studies also reported a degradation of accuracy at LW (Rudorff *et al.*, 2014; Wilson *et al.*, 2007). This deterioration is linked with an under-representation of the channels that drive the flows.

Regarding the horizontal accuracy, for WL higher than 15 m (Table 3), TS remains high (TS> 90). This result is superior to ones yielded by other hydraulics studies in the AB: 73 for Wilson *et al.*, (2007), 84 for Rudorff *et al.*, (2014). The positive BIAS suggests the model slightly over-estimates. At FW, with a WL below 15 m, TS drops down to 67, with increased positive BIAS (20). The Landsat-deduced inundation for such WL should overestimate the reality. The other explication that for WL<15m, the model present difficulties in draining due to an underrepresentation of the little channels (Rudorff *et al.*, 2014).

Table 2. WL vertical accuracy assessment

	All Station	In situ station	Virtual station	LW	RW	HW	FW
Cor. Coef.	0.99	0.99	0.99	0.32	0.99	0.95	0.99
RMSE (m)	0.27	0.28	0.27	0.48	0.12	0.20	0.34
NSE	0.99	1.00	0.99	-0.40	0.99	0.73	0.96

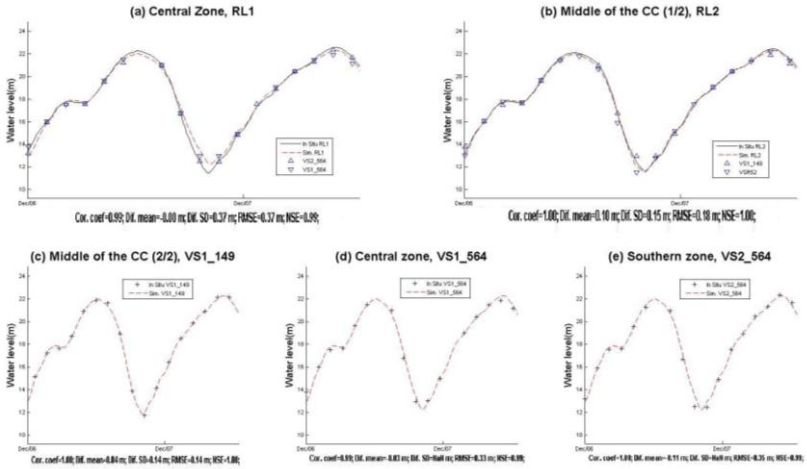

Fig. 2. WL comparisons graphics at the different places with statistics indexes: a) at RL1, b) at RL2, c) at VS1_149, d) VS1_564, e) VS2_564

Table 3. Results of horizontal accuracy

Hydrologic period	Inundation map	Date	RL1 WL (m)	TS	BIAS
LW	Landsat	--	--	--	--
ERW	DEM	02/09/2008	17.98	90.33	4.91
LRW	DEM	05/08/2008	21.38	96.70	0.19
HW	DEM	06/20/2008	22.58	97.53	-0.21
FW	Landsat 5TM	09/21/2007	14.85	64.39	20.02

1.1. Slope analysis of the mainstream

We analyse the mainstream slope between the upstream gauge (Manacapuru) and the downstream gauge (Iranduba) (Fig. 3). The WSD varies along an hydrological year: from 82 (i.e. 2.00 $cm.km^{-1}$) cm at LW to 118 cm (i.e.2.88 $cm.km^{-1}$) at RW, with an average slope of 2.55 $cm.km^{-1}$. Through altimetry, Santos *et al.* (2010) computed a slope of 2.05 $cm.km^{-1}$.

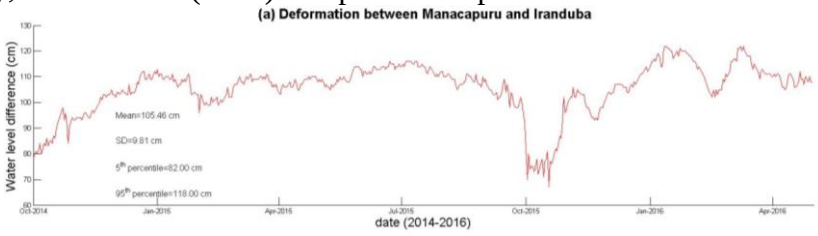

Fig. 3. Mainstream WSD

1.2. Comparison between observed and simulated data

The altimetry and the *in situ* data allow analyzing the WSD: between FP (RL1) and CC (RL2), SS (VS2_564) and CC (RL2) and inside the SS (VS2_564 and RL1). It appears that the comparison does not lead to a conclusive comparison (Table 4). Correlation remains low (value below 0.33). RMSE ranges from 16.16 cm to 40.18 cm (for an average local tidal of 1160 cm). The averaged range of obseved WSD is 49.28 cm, whereas the model predicts WSD with a magnitude of the meter (1.24 m). This result is likely due to error of the model at LW (Fig. 4). When restraining the model to RW, HW and FW, the WSD drops down to 10.72 cm. In the SS, the model predicts very low WSD. Nevertheless, several cautions regarding both simulated and observed data have to be taken into account. The true WSD should be between these two interpretations. Oberved data came from altimetry (accuracy ∓42 cm) and *in situ* gauges levelled and corrected by altimetry (accuracy ∓15 cm). Altimetry, such as *in situ* gauge, are also less precise at LW, when occurs the higher slopes in the FP. Otherwise, the model is also based on various estimations that can influence the

WL: e.g. manning coefficients, turbulence processes, evaporation, incertitudes in the boundary condition (Pinel et al., In Submission).

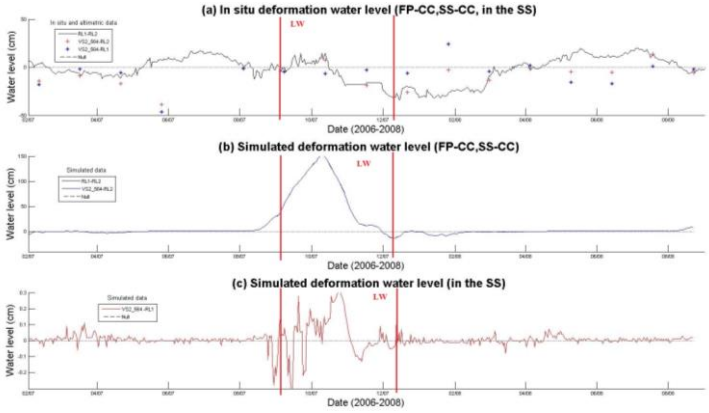

Fig. 4. a) Obs. WSD (FP-CC, SS-CC, In the SS), b)Sim. WSD (FP-CC, SS-CC), c) Sim. WSD (In the SS)

Table 4. Comparaison between observed and simulated WSD

	Between FP (RL1) and CC (RL2)	Between SS (VS2_564) and CC (RL1)	Inside the SS (VS2_564 and RL1)
Corr. coef	0.08	0.33	-0.08
RMSE (cm)	36.63	40.18	16.16
Obs. Range (cm)	45.84	46.92	55.08
Sim. range* (cm)	124 (16.05)	119 (16.03)	0.00 (0.08)

Sim. range*=Valor between parenthesis is the value obteinaed when restraining the data to RW, HW and FW

1.3. Along an hydrologic year

At LLW and ELW, (Fig. 5a, 5f, 6a and 6b), the CC acts as an outlet. The averaged WSD in this zone is 15 cm (i.e. 2.14 cm.km^{-1}) for LLW and 140 cm (20 cm.km^{-1}) for ELW. The latter number is to be manipulated with caution as the model differs from the reality during ELW: it maintains the connection between the FP and the mainstream. Nevertheless, we can expect, larger WSD during ELW than during LLW attributed to a higher WL difference between FP and river when the connection is maintened. In the rest of the FP, the WSD remain inferior to 0.4 cm and are higher in the lake than in the SS.

At ERW (Fig. 5b, 6a and 6b), the CC, acting as an inlet, drives the water from the river to the lake and the SS with low slope (0.10 cm.km^{-1}). The WSD over the whole FP is 13.81 cm. In the Lake and in the SS, the WSD remain inferior to 1 mm.

At LRW and HW (Fig. 5c, 5d, 6a and 6b), when the overbank flow occurs, the CC acts as an outlet. Inundation, in both cases, reaches almost at its maximum extension (50% of the whole watershed) the WSD over the FP WSD is 12.14 cm at LRW and 6.34 cm at HW. Nevertheless, the WSD zonal study shows the WSD over the lake and the SS is below 1 mm, and the CC record most of the WSD. This leds to slopes of 1.74 cm.km^{-1} at LRW to 0.91 cm.km^{-1} in the CC.

At FW (Fig. 5e, 5a and 6b), the overflow ceases. CC continues as an outlet with WSD of 38 cm (i.e. 5.57 cm.km^{-1}). The other parts of the flooplain present similar range of WSD (0.25 cm). Despite the water input through overflow dramatically reduces, FP exportation remains high. At this period, the backwater effect resulting from the mainstream diminishes since the WL in the latter is lower than in the FP. This can explain the increase of the slope in the CC.

1.1. Wind Incidence

In the lake zone, wich present lager dimension, the wind effect is visible in the lake: the disturbtion of the water level improves from 0.4 cm to 1.4 cm at HW and from 0.00 cm to 0.11 cm at LW. The wind influence is not so obvious in the CC and in the SS. This is likely due to the form of the latter as they are sharper, preventing the wind from spreading.

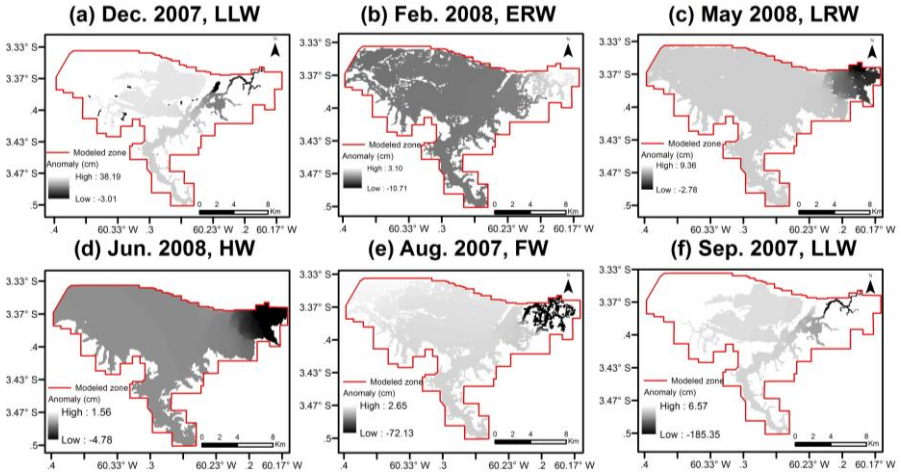

Fig. 5. WSD at different period of the hydrologic year

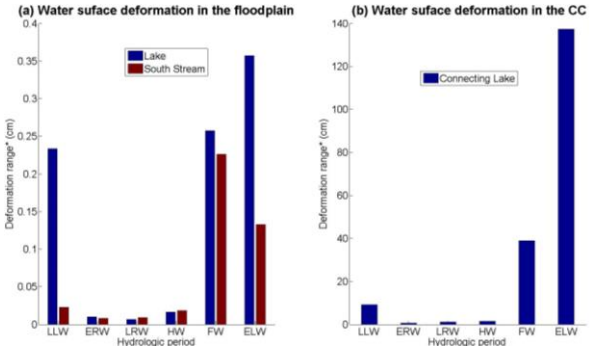

Fig. 6. WSD along an hydrologic year: a) in the lake and in the SS, b) in the CC

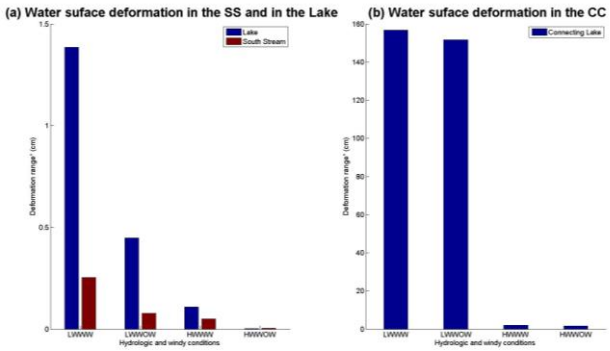

Fig. 7: Wind impact on the WSD in the FP: a) over the lake and the SS b) in the CC

4. SUMMARY AND CONCLUSIONS

The 3D hydrodynamics simulations yield new information on Amazon FP hydraulics. We use a calibrated 2D (3D averaged) model of an Amazonian FP (Janauacá Lake, Amazon State, Brazil) to analyse the WSD. We firstly validate the model: i) in term of vertical accuracy: correlation and NSE remain hight with values of 0.99 and 0.99, respectively. The global RMSE is 0.27 m (compared to a WL fluctuation of 11.60 m); ii) in terms of horizontal accuracy: the model well succeed in retrieving the flood extents (TS is 87), with a slight trend to overestimation (BIAS of 6).

The slope analysis in the mainstream in front of the study zone reports slopes varying from 2.00 $cm.km^{-1}$ at LW to 2.88 $cm.km^{-1}$ at HW. In the FP, our investigation shows that the range of observed WSD ($\mp$49 cm) is higher than the simulated ones ($\mp$11 cm). This discrepancy can be linked to incertitude on both datasets. We partition the FP in three zones (Lake, SS and CC). The model predicts important slope variations in the CC. At ERW, the CC acts as an inlet with a low reversed slope (0.01 $cm.km^{-1}$). For the other periods, slope varies from 0.17 $cm.km^{-1}$ at LRW to 19.61 $cm.km^{-1}$ at LW. Nevertheless, the latter value is likely overestimated as the model does not

simulate the full disconnection between the mainstream and the FP that actually happen. In the rest of the FP, the WSD are below 1 mm, except for LW and FW where the model predicts that the WSD are slighty higher: between 0.25 cm and 0.40 cm in the lake, respectively and between 0.15 cm and 0.25 cm in the SS, respectively. Due to higher dimensions, the wind majoritary impacts the elevation in the lake: from 0.4 cm to 1.4 cm at HW, from 0.00 cm to 0.10 cm at LW

The on-going Sentinel series, the future mission of SWOT spotlight there is now a real will of space agencies to fortify the support satellite missions can offer over water monitoring. This work stress out how hydrodynamics simulation can now be used as a support to pre-evaluate the precision expected by these sentelites mission to be exploited over the Amazonian FP.

5. ACKNOWLEDGMENTS

This research was conducted in the framework of the CNPq (*Conselho Nacional de Desenvolvimento Científico e Tecnológico*, Brazil) and IRD (*Institut de Recherche pour le Developpement*) nº 490634/2013-3, and LMI OCE (Laboratoire Mixte International Observatoire des Changements Environementaux). The first author is grateful to CAPES (*Coordenação de Aperfeiçoamento de Pessoal de Nível Superior*) in Brazil for financial support.

6. REFERENCES AND NOTES

Arcement Jr, G. J., & Schneider, V. R. (1989). Guide for Selecting Manning's Roughness Coefficients for Natural Channels and Flood Plains. *Technical Report, Geological Survey Water-Supply, United States Government Printing Office, Washington, U.S.A*, 38.

Biancamaria, S., Lettenmaier, D. P., & Pavelsky, T. (2016). The SWOT Mission and Its Capabilities for Land Hydrology. *Surveys in Geophysics*.

Bonnet, M. P., Garnier, J., Barroux, G., Boaventura, G. R., & Seyler, P. (2016). Biogeochemical Functioning of Amazonian Floodplains: The Case of Lago Grande de Curuai. In Riparian Zones: Characteristics, Management Practices and Ecological Impacts. In *Spring* (Environmen, Vol. 14, pp. 1–14). Nova publishers.

Bonnet, M. P., Pinel, S., Garnier, J., Bois, J., Bonaventura, G., & Seyler, P. (2017). Amazonian floodplain water balance based on hydrologic and electrical conductivity data analyses and modelling, (November), 1–38.

ESA. (2016). *Copernicus Market report*. http://doi.org/10.2873/827100

Fragoso, C. R., Van Nes, E. H., Janse, J. H., & da Motta Marques, D. (2009). IPH-TRIM3D-PCLake: A three-dimensional complex dynamic model for subtropical aquatic ecosystems. *Environmental Modelling and Software*, *24*(11), 1347–1348.

Grimaldi, S., Li, Y., Pauwels, V. R. N., & Walker, J. P. (2016). Remote Sensing-Derived Water Extent and Level to Constrain Hydraulic Flood Forecasting Models: Opportunities and Challenges. *Surveys in Geophysics*, *37*(5), 977–1034.

IBGE. (2016). http://www.cidades.ibge.gov.br

Junk, W., & Wantzen, K. M. (2004). The flood pulse concept: new aspects, approaches and applications - an update. In *Proceedings of the Second International Symposium on the Management of Large Rivers for Fisheries* (Vol. II, pp. 117–149).

Mangiarotti, S., Martinez, J. M., Bonnet, M. P., Buarque, D. C., Filizola, N., & Mazzega, P. (2013). Discharge and suspended sediment flux estimated along the mainstream of the Amazon and the Madeira Rivers (from in situ and MODIS Satellite Data). *International Journal of Applied Earth Observation and Geoinformation*, *21*, 341–355. http://doi.org/10.1016/j.jag.2012.07.015

Marengo, J. a, Tomasella, J., Alves, L. M., Soares, W. R., & Rodriguez, D. A. (2011). The drought of 2010 in the context of historical droughts in the Amazon region. *Geophysical Research Letters*, *38*(12), n/a-n/a. http://doi.org/10.1029/2011GL047436

Nepstad, D., McGrath, D., Stickler, C., Alencar, A., Azevedo, A., Swette, B., … Hess, L. (2014). Slowing Amazon deforestation through public policy and interventions in beef and soy supply chains. *Science*, *344*(6188), 1118–23.

Nobre, C. a, Obregón, G. O., Marengo, J. a, Fu, R., & Poveda, G. (2013). Characteristics of Amazonian Climate: Main Features. In *Amazonia and Global Change* (pp. 149–162).

Paiva, R. C. D., Collischonn, W., & Bonnet, M. P. (2012). On the sources of hydrological prediction uncertainty in the Amazon. *Hydrology and Earth System Sciences*, *16*, 1–20.

Paiva, R. C. D., Collischonn, W., & Buarque, D. C. (2011). Validation of a full hydrodynamic model for large-scale hydrologic modelling in the Amazon. *Hydrological Processes*, *27*(3).

Paiva, R. C. D., Durand, M., & Hossain, F. (2015). Spatiotemporal interpolation of discharge across a river network by using synthetic SWOT satellite data. *Water Resour. Res.*, *51*, 430–449.

Pinel, S., Bonnet, M. P., Sampaio, T. C., Silva, J. S. Da, Fragoso, C. R. J., & Cavalcanti, J. R. (n.d.). Detailed 2D flow simulation of an Amazonian floodplain as an onset for evaluating flows exchange and velocity patterns. *Water Resources Management*.

Pinel, S., Bonnet, M. P., Santos, J., Moreira, D., Calmant, S., Satge, F., & Seyler, F. (2015). Correction of interferometric and vegetation biases in the SRTMGL1 spaceborne DEM with hydrological conditioning towards improved hydrodynamics modeling in the Amazon basin. *Remote Sensing*, 16108–16130. http://doi.org/10.3390/rs70x000x

Pinel, S., Santos, J., Marques, D. M., Cavalcanti, J. R., Fragoso, C. R., Seyler, F., & Bonnet, M. P. (2017). Remotely, usefulness of floodplain, sensed data for extreme flood event modelling: a study case from an amazonian. In *Remote Sensing of Hydrometeorological Hazards*.

Rudorff, C. D. M., Melack, J. M., & Bates, P. D. (2014). Flooding dynamics on the lower Amazon floodplain: 1. Hydraulic controls on water elevation, inundation extent, and river-floodplain discharge. *Water Resources Research*, *50*(1), 619–634. http://doi.org/10.1002/2013WR014091

Santos, J., Calmant, S., Seyler, F., Rotunno Filho, O. C., Cochonneau, G., & Mansur, W. J. (2010). Water levels in the Amazon basin derived from the ERS 2 and ENVISAT radar altimetry missions. *Remote Sensing of Environment*, *114*(10), 2160–2181.

Wilson, M. D., Bates, P. D., Alsdorf, D., Forsberg, B. R., Horritt, M. S., Melack, J. M., … Famiglietti, J. (2007). Modeling large-scale inundation of Amazonian seasonally flooded wetlands. *Geophysical Research Letters*, *34*(15), L15404.

Xu, H. (2006). Modification of normalised difference water index to enhance open water features in remotely sensed imagery. *International Journal of Remote Sensing*, *27*(14), 3025–3033.

Yamazaki, D., Trigg, M., & Ikeshima, D. (2015). Development of a global ~90m water body map using multi-temporal Landsat images. *Remote Sensing of Environment*, *171*, 337–351.